JOURNAL OF MATERIALS SCIENCE **36** (2001) 2303–2311

$YNbO_4$-addition on the fracture toughness of ZrO_2(3Y) ceramics

SHENG-DIH YUH, YUANG-CHANG LAI, CHEN-CHIA CHOU*
Department of Mechanical Engineering, National Taiwan University of Science and Technology, Taipei, 106, Taiwan, Republic of China
E-mail: ccchou@mail.ntust.edu.tw

HSIN-YI LEE
Synchrotron Radiation Research Center, Hsinchu 335, Taiwan, Republic of China
E-mail: hylee@alpha1.srrc.gov.tw

Effect of $YNbO_4$ addition on the fracture toughness and stress-strain characteristics of ZrO_2(3Y) ceramics was investigated using micro-indentation, X-ray diffractometry and in-situ compression-diffraction techniques in the present work. X-ray diffraction patterns show that sintering of $YNbO_4$ and ZrO_2(3Y) mixture results in formation of a solid solution, and the tetragonality of ZrO_2(3Y) ceramics increases with the content of $YNbO_4$. The ratio of 002_t to 200_t peak intensity in X-ray diffraction spectra of the specimens changes significantly after a grinding process at low fractions of $YNbO_4$ (less than 5 mol%) and approaches to a constant value as the content of $YNbO_4$ is higher than 5 mol%, implying that the addition of $YNbO_4$ reduces the domain switchability of the ZrO_2(3Y) ceramics. Fracture toughness of modified-ZrO_2(3Y) specimens with the same heat treatment conditions could be greatly enhanced by an appropriate addition of $YNbO_4$. In addition, stress-strain curves of $YNbO_4$-modified ZrO_2(3Y) specimens exhibit an extraordinary elastic behavior. Data of in-situ loading-diffraction experiment show that an unidentified stress-induced transformation occurs and the peak intensity varies with the stress conditions. Analysis of the stress-strain characteristics and X-ray diffraction results suggest that the fracture toughness of the specimens cannot be simply attributed to the t-to-m phase transformation.

1. Introduction

Since Garvie *et al*. [1, 2] firstly realize the potential of utilizing the tetragonal-to-monoclinic (t-to-m) phase transformation of metastable tetragonal zirconia for increasing both strength as well as toughness of the ceramics, the relationship between fracture toughness and phase transformation in zirconia-based ceramics has been studied extensively over the past two decades [3–10].

For partially stabilized zirconia (PSZ) and tetragonal zirconia polycrystals (TZP), the volume change and the shear strain developed in the t-to-m martensitic transformation have been recognized to oppose the opening of the crack, and hence increase the resistance to crack propagation in ceramics. This is the generally accepted toughening mechanism in the zirconia-related materials [1–10]. However, some experimental results indicated that toughening behavior in zirconia-related materials could not be simply interpreted in terms of phase transformation toughening. Ferroelastic domain switching and other behavior have recently been observed and may contribute to the fracture toughness of some zirconia-related materials [11–24]. For example, Ingel *et al*. [14, 15] observed that yttria-doped single crystals of partially stabilized zirconia exhibited fracture toughness twice in magnitude as that of fully stabilized crystals at 1100°C. Transformation toughening alone cannot account for this retention of high toughness above the monoclinic-to-tetragonal transition temperature, since the corresponding stress-induced t-to-m transformation has been shown not to be possible above approximately 900°C.[15] Michel *et al*. [16, 17] found the fracture toughness of the tetragonal single crystals of zirconia to be about 6 $MPa \cdot m^{1/2}$ and analysis of fracture surfaces of the crystals by X-ray diffraction also failed to reveal existence of the monoclinic phase, which is not in accordance with the transformation toughening mechanism. This phenomenon is observed by Tsukuma *et al*. [18] in yttria-doped polycrystalline zirconia as well. The results [11–24] indicate that transformation toughening does not fully explain the observed high toughness of the materials.

Furthermore, Virkar *et al*. [11–13] have observed that ceria-stabilized tetragonal zirconia ceramics exhibit an

* Author to whom all correspondence should be addressed.

increase in the (002) peak intensity and a simultaneous decrease in the (200) peak intensity after surface grinding. Srinivasan *et al*. [21] and Saiki *et al*. [22] observed the domains of zirconia single crystals undergoing switching after applying a stress, using an X-ray diffractometry method. Lankford *et al*. [23] have reported yttria-stabilized zirconia to exhibit two-stage yielding in the stress-strain behavior, yet, no monoclinic phase was present in the yielding process. All these results appear to suggest that the domain switching may probably be an effective toughening mechanism in zirconia-based and related materials. However, in most cases it is difficult to differentiate the effect of phase transformation from that of ferroelastic domain switching on the toughening behavior. In this paper, we report the effect of $YNbO_4$ addition on the phase assemblage, toughness and some intriguing behavior of stress-strain curves of ZrO_2(3Y) modified with $YNbO_4$ in contrast to previous works [25–27]. An endeavor to differentiate the toughening mechanisms has also been attempted.

2. Experimental

The $YNbO_4$ powders were prepared from Y_2O_3 (99.99%, Research chemicals, USA) and Nb_2O_5 (99.9%, Meldform, UK) by an oxide-mixing method, followed by calcination at 1100°C. The specimen compositions prepared were ZrO_2(3Y) (HSY-3, Daiichi, Japan) with 0 to 20 mol% $YNbO_4$. The mixtures of $YNbO_4$ and ZrO_2(3Y) were sequentially processed by wet centrifugal ball milling, vacuum drying at 60°C, calcining at 1000°C and ball milling again. The resulting powders were compressed using a cold-isostatic-press under a loading of 270 MPa to form cylindrical pellets or rods. Final specimens were obtained by sintering these pellets from 1350 to 1700°C in air for different periods [28]. X-ray diffraction measurements were made on the specimen surface and interior. To derive data from specimen interior, the specimens were cut slowly into two pieces using a diamond saw and then polished with diamond paste carefully to remove the plastically deformed layer. Phase identifications of as-sintered and fractured surfaces were performed by X-ray diffractometry (DMAX-B, Rigaku, Japan) using Cu K_α radiation and the fractions of phases in the materials were estimated employing Howard and Hill's polymorph method [29]. Mechanical property investigations were carried out after the specimens were ground, some were stress-relief heat treated and then polished. Micro-hardness measurements were carried out using a Vickers hardness tester (DVK-1S, Matsuzawa, Japan), and the fracture toughness was determined by micro-indentation technique using the equation recommended by Japanese Industry Standard (JIS R1607, 1995): $K_{IC} = 0.018(E/H)^{1/2}(P/C)^{1.5}$, where K_{IC} is the fracture toughness in unit MPa $\cdot$ m$^{1/2}$; E is the elastic modulus in unit Pa and was measured using a uniaxial compressive loading on a cylinder rod ($\phi = 6$ mm, gage length = 25 mm) with a crosshead speed of 10.0 μm/min using a dynamic material testing system (MTS 810, USA); H is the Vickers hardness; P is the indentation load in unit N and C is one half of the average length of the four corner cracks of the indent in unit μm.

In-situ high resolution X-ray diffraction measurements were carried out at the wiggler beamline BL-17B at the Synchrotron Radiation Research Center, Hsinchu, Taiwan. The electron storage ring was operated at energy of 1.5 GeV, and a current of 140–200 mA, which delivered 8.04 KeV X-ray photons with an estimated flux of 10^{10} photons/sec for this experiment. The specimens were fixed using a custom designed gripper and then put on a holder of the X-ray diffractometer. The specimens were bonded with a strain gage (Measurements Group, EA-06-250BF-350-option LE, USA) and then compressed uniaxially by a screw wrench. The strain was measured using a strain indicator (Measurements Group, P-3500, USA). *In-situ* diffraction patterns were obtained from the as-sintered, compressed and released surfaces. Grain size, specimen surface and internal structure of specimens were investigated employing a scanning electron microscope (Hitachi S800, Japan) and a transmission electron microscope (JEOL JEM-2010, Japan) with a double-tilt specimen stage.

3. Results and discussion

X-ray diffraction pattern of the $YNbO_4$ powder prepared by an oxide-mixing method and calcined at 1100°C is shown in Fig. 1, which shows that the $YNbO_4$ phase has completely formed (peaks match with JCPDS 23-1468), and some intermediate phases disappear during the sintering process.

X-ray diffraction patterns of the ZrO_2(3Y) specimens, doped with different $YNbO_4$ contents and sintered at 1600°C for 1 hour, are shown in Fig. 2. It is observed that as the amount of $YNbO_4$ is smaller than 10 mol %, the specimens exhibit no $YNbO_4$ peaks after sintering, implying that $YNbO_4$ has been completely dissolved in ZrO_2(3Y) at the present heat treatment condition. If the content of $YNbO_4$ is more than 10 mol %, undissolved $YNbO_4$ can be observed. Fig. 2 also shows that the specimens are mainly the tetragonal and the cubic phases, and the amount of the monoclinic phase is limited.

Relative densities and Vickers hardness of the modified-ZrO_2(3Y) specimens are revealed in Fig. 3.

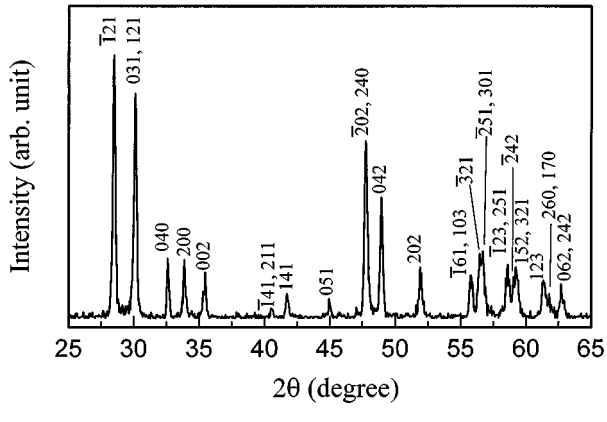

Figure 1 X-ray diffraction pattern of the $YNbO_4$ powder prepared by an oxide-mixing method and calcined at 1100°C. All peaks match with JCPDS 23-1468.

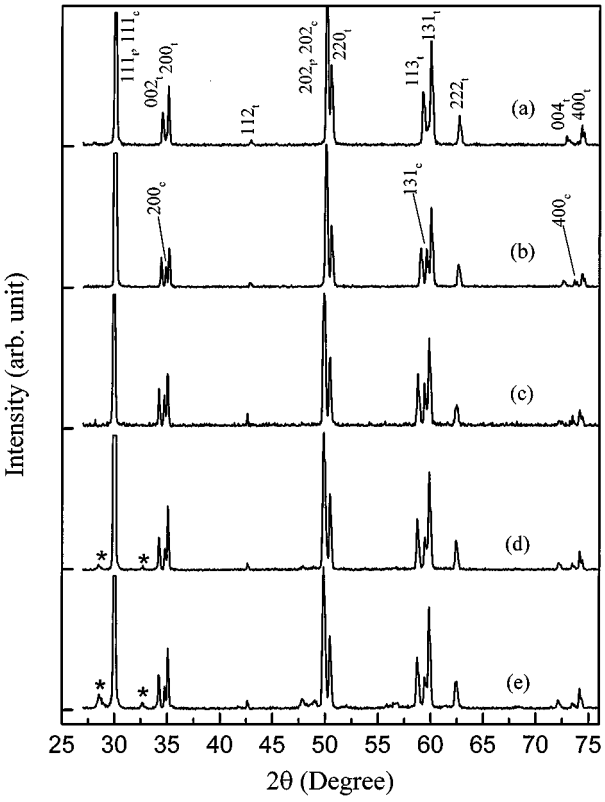

Figure 2 X-ray diffraction patterns of ZrO_2 (3Y) specimens with different $YNbO_4$ contents (a) 0, (b) 5, (c) 10, (d) 15 and (e) 20 mol % sintered at 1600°C for 1 hour. The asterisks indicate $YNbO_4$ peaks.

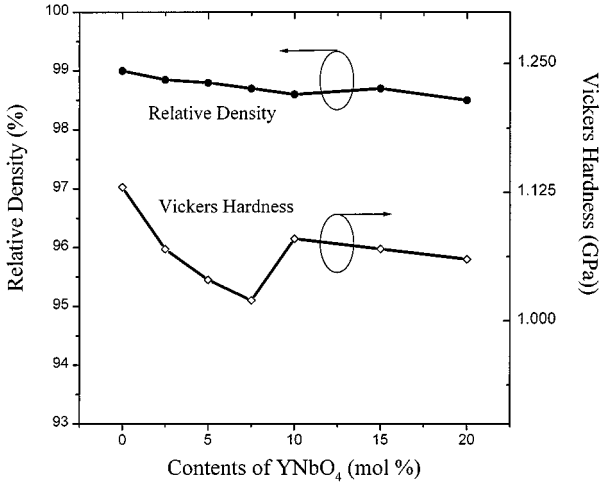

Figure 3 The relative density and the Vickers hardness of ZrO_2(3Y) specimens with different $YNbO_4$ contents sintered at 1600°C for 1 hour.

It shows that the relative density maintains higher than 98% while the Vickers hardness of the specimens show an intriguing tendency, that is, it decreases firstly and then increases as contents of $YNbO_4$ increases, showing a hardness minimum at around 5 mol % $YNbO_4$. Scanning electron micrographs of the specimens are presented in Fig. 4. It can be seen that the addition of $YNbO_4$ promotes the grain growth. Average grain sizes of specimens were calculated and summarized later.

Indentation microcrack of the specimens of ZrO_2(3Y) doped with different $YNbO_4$ contents sintered at 1600°C for 1 hour are shown in Fig. 5. Specimens with 2.5 to 5 mol % $YNbO_4$ show very small indentation cracks, which suggest that modified ZrO_2(3Y) with a suitable $YNbO_4$ concentration (around 2.5 to 5 mol%) does enhance the fracture toughness of ZrO_2(3Y) effectively.

Two possible toughening mechanisms, domain switching and t-to-m phase transformation, may work in the zirconia-based materials as described in introduction. In order to demonstrate the occurrence of domain switching in the tetragonal phase, the specimens were subjected to grinding process and the X-ray diffraction patterns of the as-sintered and the surface-ground specimens were recorded. Fig. 6 shows the X-ray diffraction peaks associated with 002_t and 200_t planes at 2θ around 34–36° in as-sintered as well as ground specimens of ZrO_2(3Y) doped with different $YNbO_4$ contents sintered at 1600°C for 1 hour. A sketch of the ratio of peak intensity, $002_t/200_t$, for the specimens before and after grinding is shown in Fig. 7, which implies that grinding induced domain switching occurs for specimens with $YNbO_4$ content smaller than 7.5 mol %. For specimens with $YNbO_4$ content higher than 7.5 mol %, domain switching was not observed, suggesting that $YNbO_4$ addition suppress domain switchability of the specimens. At the same time, we measure the phase assemblage of the fracture surface of specimens, as shown in Fig. 8. The results show that the tetragonal phase of the specimen containing 2.5 mol % $YNbO_4$ has transformed to the monoclinic phase in a large amount, while the specimen containing 10 mol % $YNbO_4$ almost shows no monoclinic phase on the fracture surface. This suggests that $YNbO_4$ addition suppress not only domain switching but also the t-to-m transformation of the specimens, as the specimens possess $YNbO_4$ content higher than 7.5 mol %.

Summary of characteristics of the specimens was drawn as a function of different $YNbO_4$ content, shown in Fig. 9. Variations of the fracture toughness is observed as the curve "K" in Fig. 9, which shows that the fracture toughness of the specimen with 2.5 mol % $YNbO_4$ is nearly 2.5 times higher than that without $YNbO_4$ addition under identical preparation conditions. The fraction of the tetragonal phase and the grain size were calculated and shown by curves "t" and "G" in Fig. 9, respectively. The c/a ratio, i.e, the tetragonality, calculated from Fig. 2 for the tetragonal phase of the specimens approaches to a saturation value, as $YNbO_4$ content increases, as shown by the curve "T" in Fig. 9.

Aliovalent cation dopants are generally believed to substitute for Zr ions in the cation network, creating oxygen vacancies for charge compensation [30]. The ensuing lattice distortion by oxygen vacancies associated with Zr provides stability to the tetragonal and cubic phases of zirconia [31]. However, the number of such oxygen vacancies increases during stabilization process, which consequently causes the tetragonality of zirconia to decrease [30]. On the other hand, in the solid solution of the tetragonal zirconia with $YNbO_4$, Y adopts a YO_8 structure with a bond length of 2.32 Å and is not associated with oxygen vacancies, while Nb adopts a NbO_4 structure with a bond length of 1.90 Å. This is shorter than the Zr-O_I distance of 2.10 Å. The strong Nb-O coordination thus

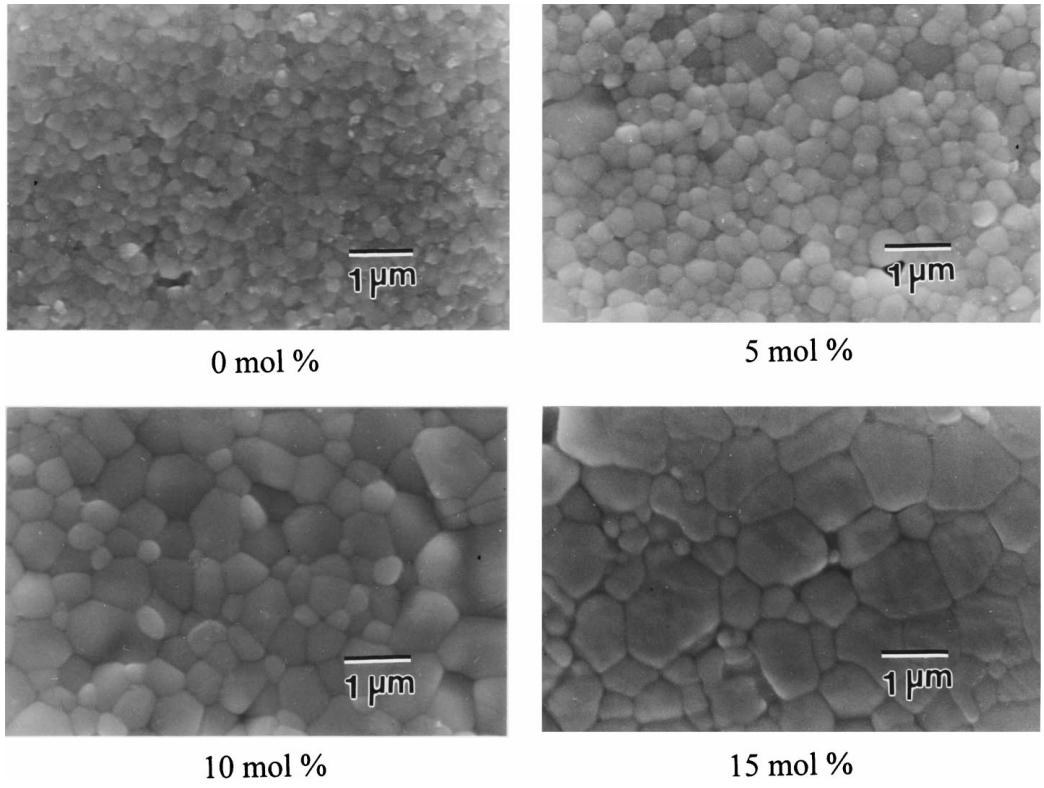

Figure 4 Scanning electron micrographs of the specimens with different $YNbO_4$ contents. The specimens were sintered at 1600°C for 1 hour.

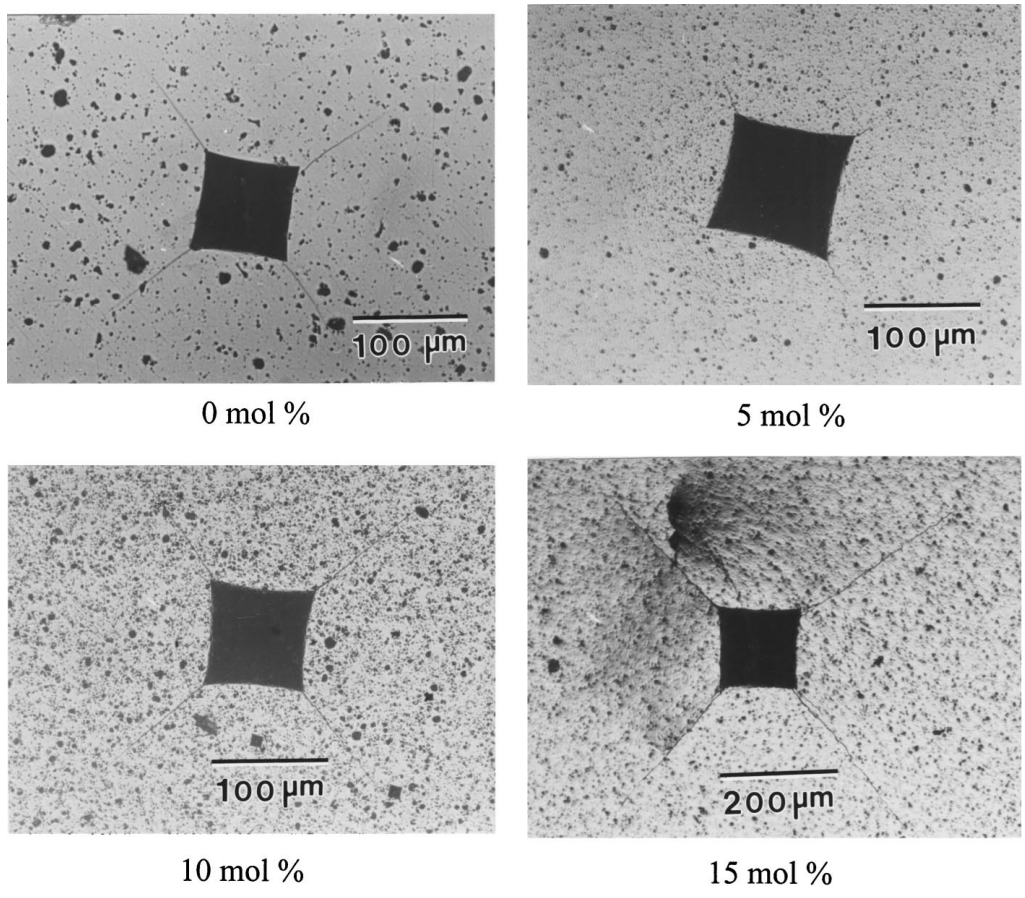

Figure 5 Indentation microcrack development in specimens with different $YNbO_4$ contents sintered at 1600°C for 1 hour.

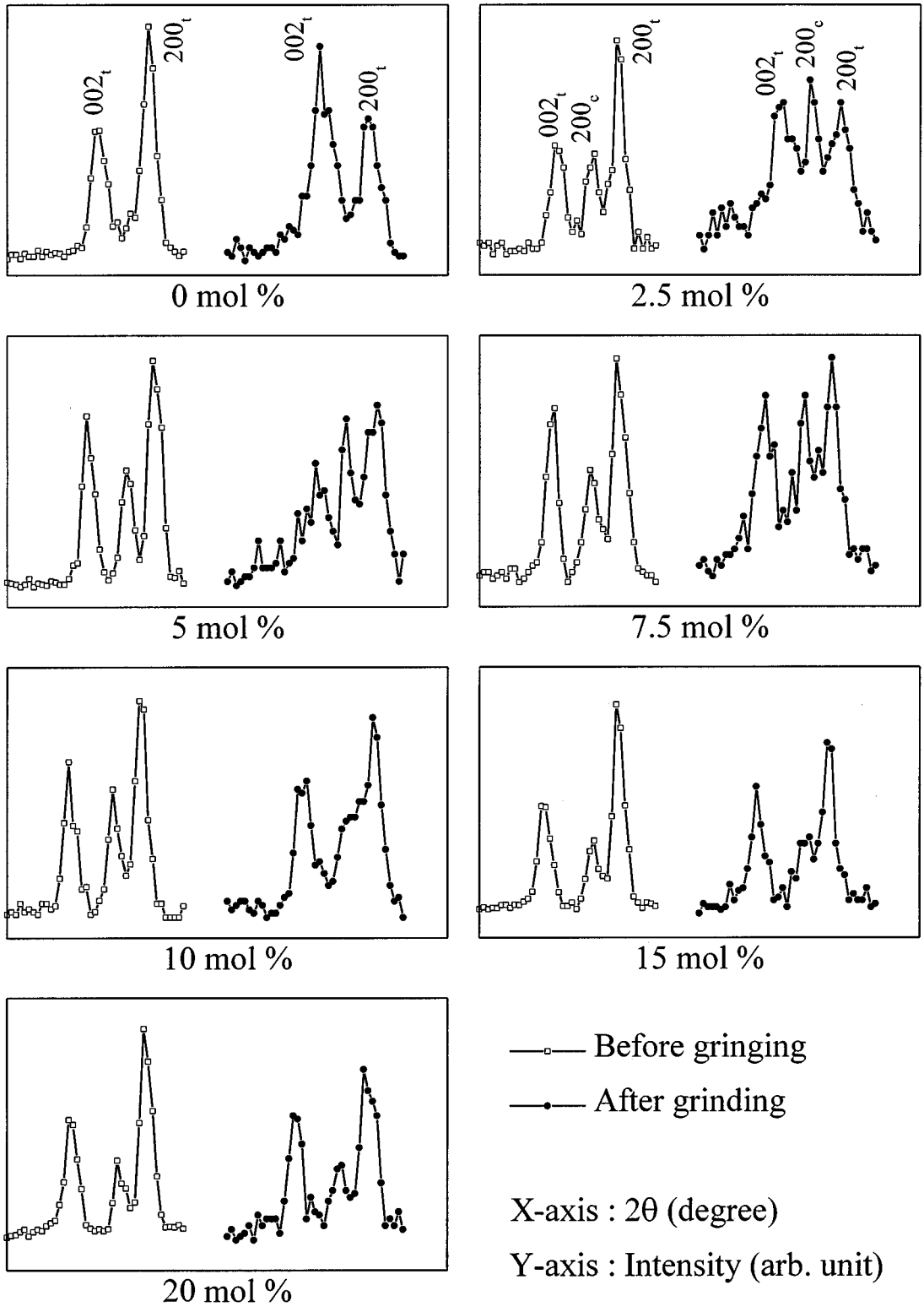

Figure 6 Expended XRD patterns for 002_t and 200_t peak intensity at $2\theta = 34$–36° for ZrO_2(3Y) specimens with different $YNbO_4$ contents. The specimens were sintered at 1600°C for 1 hour.

increases the bonding disparity between Zr-O layers, consequently increasing the tetragonality [31]. This is consistent with the present result shown by curve "T" in Fig. 9. Furthermore, it has been shown that the fracture toughness increases with increase in tetragonality in the Nb_2O_5-ZrO_2 system [32, 33]. This was explained by arguing that Nb^{5+} combines with oxygen interstitial in ZrO_2 during formation of Nb_2O_5 solid solution with ZrO_2, which reduces the concentration of the oxygen vacancies and makes the tetragonal phase unstable. It means that phase transformability from tetragonal to monoclinic increases with addition of Nb, and thus the fracture toughness enhancement appears to be simply related to a phase transformation mechanism. However, by observing Figs 7 and 9, the fracture toughness of the $YNbO_4$-doped ZrO_2(3Y) specimens decreases as the c/a ratio increases for specimens with $YNbO_4$ content higher than 5 mol %. This may be due to the chemical composition modification of the specimens showing constant oxygen vacancy concentration, which is

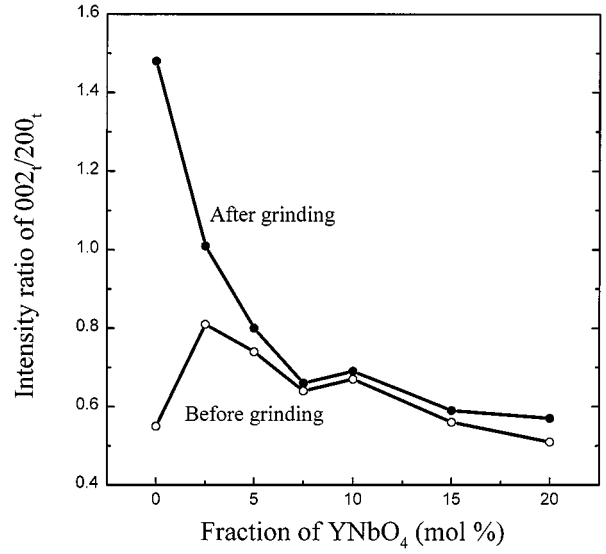

Figure 7 Intensity ratio of the peaks $002_t/200_t$ for ZrO_2(3Y) specimens with different $YNbO_4$ contents before and after grinding. The specimens were sintered at 1600°C for 1 hour.

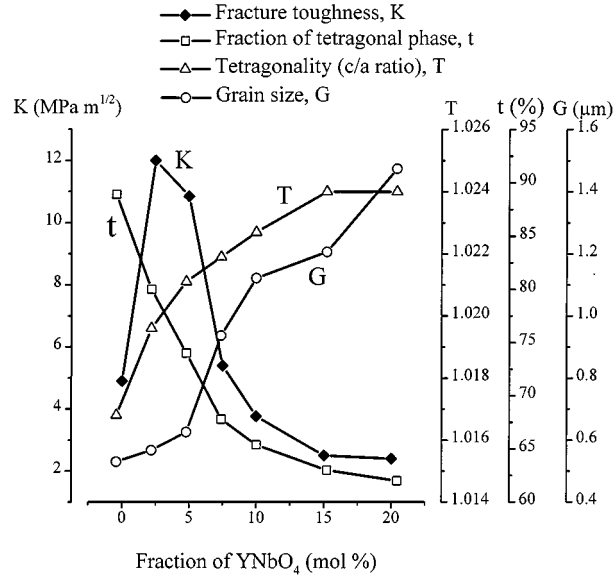

Figure 9 Variations in fracture toughness, tetragonality, fraction of the tetragonal phase and grain size for specimens with different $YNbO_4$ contents. The specimens were sintered at 1600°C for 1 hour.

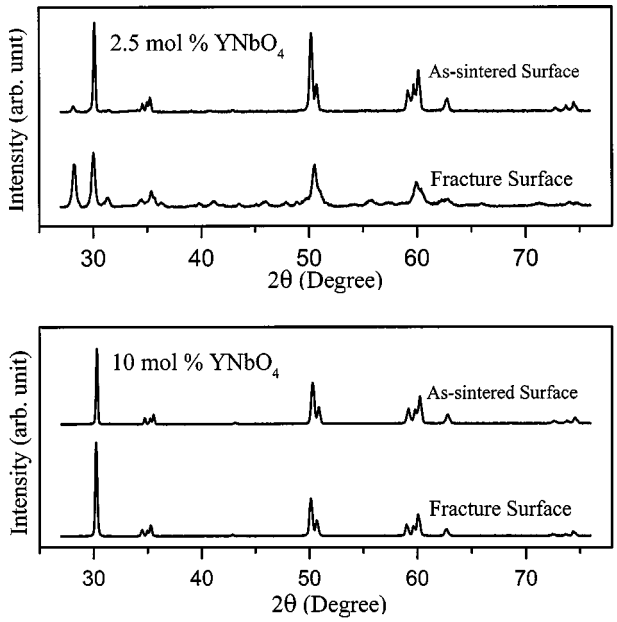

Figure 8 The changes of the diffraction peak before and after fracture of the ZrO_2(3Y) specimen doped with 2.5 and 10 mol % $YNbO_4$. The specimens were sintered at 1600°C for 1 hour.

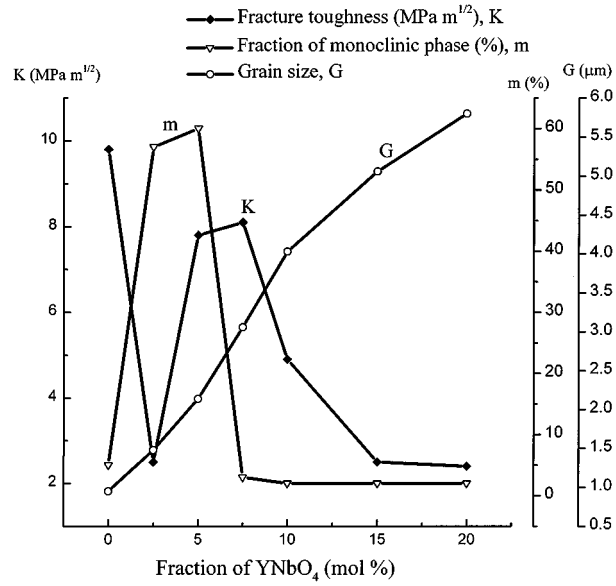

Figure 10 Fraction of the monoclinic phase, fracture toughness and grain size for ZrO_2(3Y) specimens (as-sintered) with different $YNbO_4$ contents sintered at 1600°C for 10 hours.

different from that of the Nb_2O_5-ZrO_2 system, and may be attributed to the stabilization of the tetragonal phase in the present material system.

Fracture toughness of a tetragonal zirconia polycrystal is strongly dependent on the grain size [34]. The tetragonal phase becomes easier to transform when grain size of a specimen increases. Contribution of t-to-m transformation to fracture toughness contribution at a constant temperature therefore increases [35]. To verify the grain size and the composition homogeneity effects, ZrO_2(3Y) specimens doped with different $YNbO_4$ contents sintered at 1600°C for 10 hours were investigated. Again, we observe that the addition of $YNbO_4$ promotes the grain growth. The fracture toughness of the specimens and the corresponding fraction of the monoclinic phase are shown in Fig. 10. The ZrO_2(3Y) specimen show a prominent increase in fracture toughness due to the grain size effect on transformability. Fig. 10 provides an interesting result indicating that t-to-m transformation may not be the only toughening mechanism for the specimens. That is, although fraction of the monoclinic phase in the 5 mol% $YNbO_4$ specimen is as high as 60%, the specimen still exhibits a nearly highest value of the fracture toughness. On the other hand, as 2.5 mol% $YNbO_4$ was added in the specimen, a large amount of the monoclinic phase was introduced but a rapid drop of the fracture toughness of the specimen was observed. Intriguingly, grain size of the specimen with 5 mol%

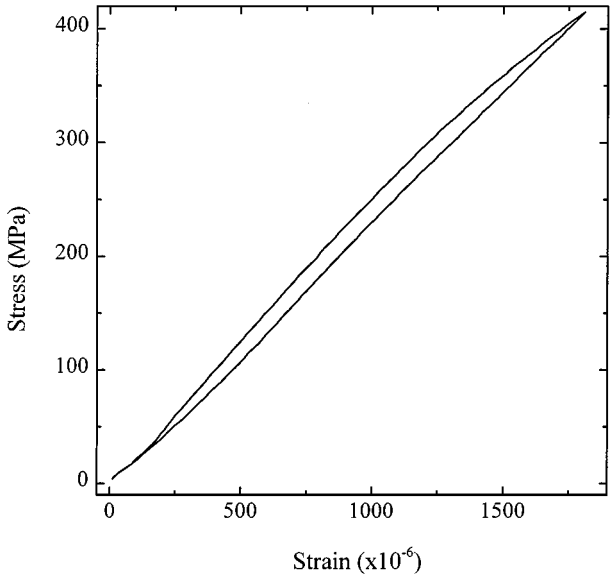

Figure 11 An axial stress-strain curve of ZrO_2(3Y)-5 mol%$YNbO_4$ specimens sintered at 1600°C for 1 hour under a compression test showing hysteresis loops without permanent strain.

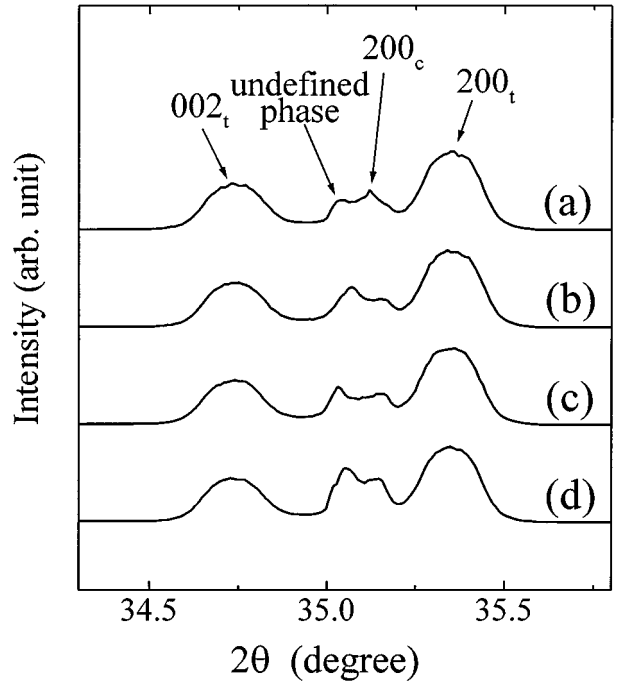

Figure 12 The variation of the diffraction peaks under *in-situ* uni-axial compression loading of the ZrO_2-5 mol%$YNbO_4$ specimen sintered at 1600°C for 1 hr. (a) initial state, (b) 1000 $\mu\varepsilon$, (c) 2000 $\mu\varepsilon$ and (d) released condition.

$YNbO_4$ is larger than that of the specimen with 2.5 mol% $YNbO_4$. This suggests that $YNbO_4$ addition with amounts smaller than or around 5 mol% not only greatly enhance grain growth, but also modify the t-to-m transformation characteristics. The tetragonal phase of a specimen may have transformed into the monoclinic phase in a large amount, but the fracture toughness of the specimens does not necessarily decay. This high toughness of the ZrO_2(3Y) specimen with 5 mol% $YNbO_4$ can not be simply explained by a t-to-m phase transformation mechanism, since a large amount of the tetragonal phase have transformed into the monoclinic phase. Origin of this high toughness therefore may probably be attributed to domain switching or other mechanisms. In addition, when the $YNbO_4$ addition is higher than 7.5 mol %, increasing in tetragonality of the specimens suppresses the phase transformability and makes toughness of the $YNbO_4$-doped specimens decrease, indicating that phase transformation induced volume change and therefore the compressive stress do play a role in toughness enhancement.

Enhancement of the energy absorbing capability of a brittle material can be observed by the increase of its ductility. Fig. 11 shows the stress-strain curves of a cylindrical specimen of ZrO_2(3Y)-5 mol%$YNbO_4$ sintered at 1600°C for 1 hour in a compression experiment under a loading of 415 MPa. Intriguingly, the compressed specimen exhibited a hysteresis loop at the axial direction in the stress-strain curve during loading-unloading process. The strain recovers completely after unloading. This kind of pseudoelastic behavior is ordinarily attributed to a reversible stress-induced-transformation or a ferroelastic behavior of the materials [36]. Materials containing a reversible stress-induced phase transformation show large pseudoelastic strains due to a structural change during a phase transition [36]. Ferroelastic materials often exhibit high elastic deformation and often contain movable domain boundaries which soften the materials [37–39]. The area enclosed by the hysteresis loops shown in Fig. 11, could be the mechanical energy stored in the material in a loading cycle due to either a ferroelastic behavior [11] or a stress-induced-transformation [36].

To verify either a ferroelastic behavior or a stress-induced-transformation in the material, an *in-situ* high resolution diffractometry for uniaxial compression experiments using synchrotron radiation was conducted. The intensity variations of diffraction patterns during loading and unloading procedures under a uniaxial compression of rectangular specimen ZrO_2(3Y) doped with 5 mol % $YNbO_4$ sintered at 1600°C for 1 hour are shown in Fig. 12. At the initial loading-free condition, two peaks exist between 002_t and 200_t. One of these two peaks is cubic phase 200_c which is originally subsistent in $YNbO_4$-doped ZrO_2(3Y) specimens, and the other is an unidentified phase which was not reported to exist in ZrO_2(3Y) specimens. The formation of this unidentified phase in the present material system is because of the $YNbO_4$-addition. Intriguingly, the peak intensity of this phase varies with the stress condition under the condition of no apparent changes in intensity of the tetragonal peaks of 002_t and 200_t. That is, the result indicates that an stress-induced transformation rather than t-to-m transformation or a stress-induced domain switching occur in the present material system.

In addition to the well-known cubic, tetragonal and monoclinic polymorphs of the zirconia, this extra phase can be confirmed by transmission electron microscopy. Fig. 13 shows the morphology and the corresponding diffraction pattern of a specimen of ZrO_2(3Y) doped with 5 mol % $YNbO_4$ sintered at 1600°C for 1 hour. Note that around the principal reflections, which were analyzed to be the monoclinic twins and the tetragonal

(a)

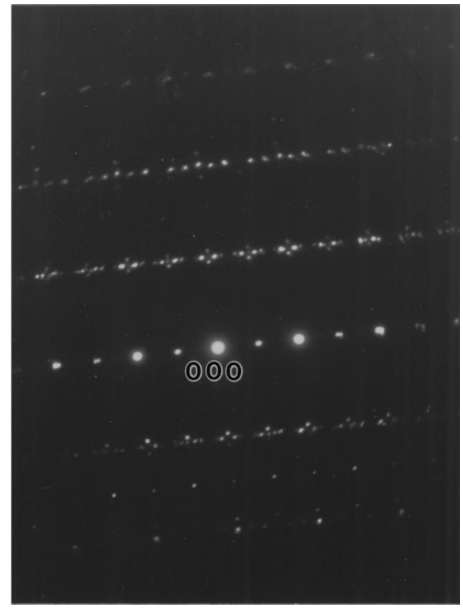

(b)

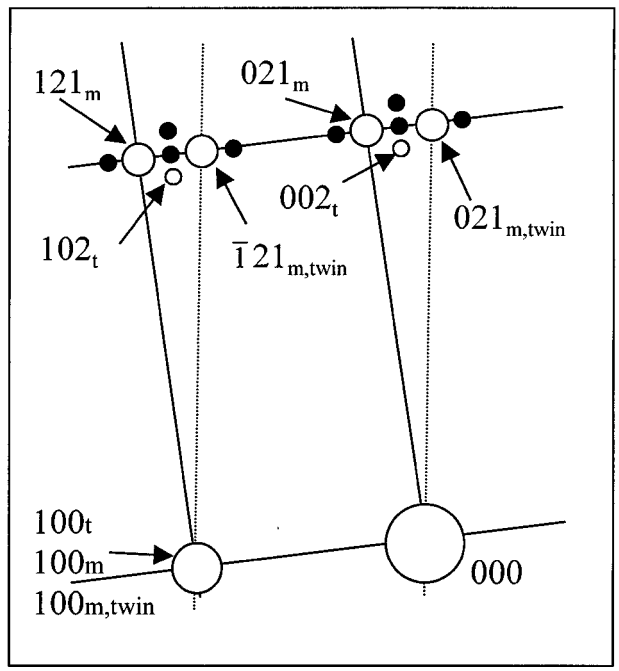

(c)

Figure 13 TEM micrograph showing (a) a bright field image with complicated internal structures, (b) the corresponding diffraction pattern and (c) indices showing a zone axis of [010] for the tetragonal phase, [01$\bar{2}$] for the monoclinic phase and some spots for undefined (indicated by solid circle) phases.

phase, fine and weak extra spots were observed. These extra spots can not be ascribed to the cubic, the tetragonal and the monoclinic phases and preliminary analyses indicate that the phase may probably be the orthorhombic and/or rhombohedral phases, but the peak positions do not match very well with those reported in the previous works [40–42].

4. Conclusions

The effect of $YNbO_4$ addition on fracture toughening of ZrO_2(3Y) ceramics was investigated. The main results are summarized as follows:

1. Sintering of $YNbO_4$ and ZrO_2(3Y) mixture results in a solid solution with $YNbO_4$ content smaller

than 10 mol%, and tetragonality of ZrO_2(3Y) ceramics increases with the content of $YNbO_4$. Addition of $YNbO_4$ promotes grain growth of the specimens and stabilizes the tetragonal phase effectively.

2. The intensity of $(002)_t$ and $(200)_t$ peaks changes greatly at low fractions of $YNbO_4$ (0 and 2.5 mol%) after grinding, while it saturates with further increase in the content of $YNbO_4$. Phase assemblage of the fracture surface of specimens shows that the t-to-m transformation occurs more easily for the specimen containing lower content of $YNbO_4$. The result implies that addition of $YNbO_4$ reduces the domain switchability and the phase transformability of the ZrO_2(3Y) ceramics.

3. Fraction of the monoclinic phase in the $ZrO_2(3Y) + 5$ mol % $YNbO_4$ specimen sintered at 1600°C for 1 hour is as high as 60%, the specimen still exhibits a nearly highest value of the fracture toughness. On the other hand, as 2.5 mol % $YNbO_4$ was added in the specimen, a large amount of the monoclinic phase was introduced but a rapid drop of the fracture toughness of the specimen was observed. Intriguingly, grain size of the specimen with 5 mol% $YNbO_4$ is larger than that of the specimen with 2.5 mol % $YNbO_4$. This suggests that $YNbO_4$ addition with amounts smaller than or around 5 mol % not only greatly enhance grain growth, but also modify the t-to-m transformation. The tetragonal phase of a specimen may have transformed into the monoclinic phase in a large amount, but the fracture toughness of the specimens does not necessarily decay.

4. Fracture toughness of modified-ZrO_2(3Y) specimens with the same heat treatment conditions could be greatly enhanced by an appropriate addition of $YNbO_4$. In addition, stress-strain curves of $YNbO_4$-modified ZrO_2(3Y) specimens exhibit an extraordinary elastic behavior. Data of *in-situ* compression-diffraction experiment show that an unidentified stress-induced transformation occurs and the peak intensity varies with the stress conditions. Analysis of the stress-strain characteristics and X-ray diffraction results suggest that the fracture toughness of the specimens can not be simply attributed to the t-to-m phase transformation.

Acknowledgement

This paper is supported by the National Science Council of Taiwan, Republic of China, under project No. NSC89-2216-E-011-026.

References

1. R. C. GARVIE, R. H. HANNINK and R. T. PASCOE, *Nature* **258** (1975) 703.
2. R. C. GARVIE and P. S. NICHOLSON, *J. Amer. Ceram. Soc.* **55** (1972) 152.
3. A. G. EVANS and R. M. CANNON, *Acta Metall.* **34** (1986) 761.
4. F. F. LANGE, *J. Mater. Sci.* **17** (1982) 255.
5. D. L. PORTER and A. H. HEUER, *J. Amer. Ceram. Soc.* **60** (1977) 183.
6. *Idem., ibid.* **62** (1979) 298.
7. A. H. HEUER, N. CLAUSSEN, W. M. KRIVEN and M. RUHLE, *J. Amer. Ceram. Soc.* **65** (1982) 642.
8. A. H. HEUER and M. RUHLE, in "Science and Technology of Zirconia II," edited by N. Claussen, M. Ruhle and A. H. Heuer (American Ceramic Society, Columbus, OH, 1984) p. 1.
9. E. STEVENS, in "Zirconia and Zirconia Ceramics" (Magnesium Elektron, Flemington, New Jersey, 1986) p. 1.
10. A. H. HEUER and M. RUHLE, in "Advances in Ceramics" Vol. 12, Science and Technology of Zirconia II, edited by N. Claussen, M. Ruhle and A. H. Heuer (American Ceramic Society, Columbus, OH, 1984) p. 137.
11. A. V. VIRKAR and R. L. K. MATSUMOTO, *J. Amer. Ceram. Soc.* **69** (1986) C-224.
12. A. V. VIRKAR and R. L. K. MATSUMOTO, in "Science and Technology of Zirconia III," edited by S. Somiya, N. Yamamoto and H. Yanagida (American Ceramic Society, Westerville, OH, 1988) p. 653.
13. C. J. CHAN, F. F. LANGE, M. RUHLE, J. F. JUE and A. V. VIKAR, *J. Amer. Ceram. Soc.* **74** (1991) 807.
14. R. P. INGEL, D. LEWIS, B. A. BENDER and R. W. RICE, in "Science and Technology of Zirconia II," edited by N. Claussen, M. Ruhle and A. H. Heuer (American Ceramic Society, Columbus, OH, 1984) p. 408.
15. R. P. INGEL, D. LEWIS, B. A. BENDER and R. W. RICE, *J. Amer. Ceram. Soc.* **65** (1982) C-150.
16. D. MICHEL, L. MAZEROLLES and M. P. JORBA, *J. Mater. Sci.* **18** (1983) 2618.
17. D. MICHEL, L. MAZEROLLES and M. P. JORBA, in "Science and Technology of Zirconia II," edited by N. Claussen, M. Ruhle and A. H. Heuer (American Ceramic Society, Columbus, OH, 1984) p. 131.
18. T. TSUKUMA, Y. KUBOTA and T. TSUKIDATE, in "Science and Technology of Zirconia II," edited by N. Claussen, M. Ruhle and A. H. Heuer (American Ceramic Society, Columbus, OH, 1984) p. 382.
19. K. MEHTA, J. F. JUE and A. V. VIRKAR, *J. Amer. Ceram. Soc.* **73** (1990) 1777.
20. M. G. CAIN and M. H. LEWIS, *Mater. Lett.* **9** (1990) 309.
21. G. V. SRINIVASAN, J. F. JUE, S. Y. KUO and A. V. VIRKAR, *J. Amer. Ceram. Soc.* **72** (1989) 2098.
22. A. SAIKI and N. MIZUTANI, *Trans. Mat. Soc. Jpn.* **14A** (1994) 451.
23. J. LANKFORD, R. A. PAGE and L. RABENBERG, *J. Mater. Sci.* **23** (1988) 4144.
24. K. MEHTA and A. V. VIRKAR, *J. Amer. Ceram. Soc.* **73** (1990) 567.
25. V. S. STUBICAN, *ibid.* **47** (1964) 55.
26. P. LI, I. W. CHEN and J. E. PENNER-HAHN, *ibid.* **77** (1994) 1289.
27. T. D. KETCHAM, U. S. Patent 5008221 (1991).
28. T. SATO and M. SHIMADA, *J. Amer. Ceram. Soc.* **68** (1985) 356.
29. C. HOWARD and R. J. HILL, *J. Mater. Sci.* **26** (1991) 127.
30. P. LI, I. W. CHEN and J. E. PENNER-HAHN, *J. Amer. Ceram. Soc.* **77** (1994) 118.
31. P. LI, I. W. CHEN and J. E. PENNER-HAHN, *ibid.* **77** (1994) 1281.
32. D. J. KIM, *ibid.* **73** (1990) 115.
33. D. J. KIM, P. F. BECHER and C. R. HUBBARD, *ibid.* **76** (1993) 2904.
34. M. V. SWAIN, *J. Mater. Sci. Letter* **5** (1986) 1159.
35. P. F. BECHER, *J. Amer. Ceram. Soc.* **75** (1992) 493.
36. K. OTSUKA and K. SHIMIZU, *Metals Forum.* **73** (1981) 142, and references therein.
37. J. LI and C. M. WAYMAN, *J. Amer. Ceram. Soc.* **80** (1997) 803.
38. T. L. BAKER, K. T. FABER and D. W. READEY, *ibid.* **74** (1991) 1619.
39. V. K. WADHAWAN, *Phase Transitions.* **3** (1982) 3.
40. T. A. BIELICKI, U. DAHMEN, G. THOMAS and K. WESTMACOTT, in "Science and Technology of Zirconia III," edited by S. Somiya, N. Yamamoto and H. Yanagida (American Ceramic Society, Westerville, OH, 1988) p. 485.
41. B. C. MUDDLE and R. H. J. HANNINK, in "Science and Technology of Zirconia III," edited by S. Somiya, N. Yamamoto and H. Yanagida (American Ceramic Society, Westerville, OH, 1988) p. 89.
42. H. HASEGAWA, *J. Mater. Sci. Lett.* **2** (1983) 91.

Received 19 January
and accepted 25 October 2000